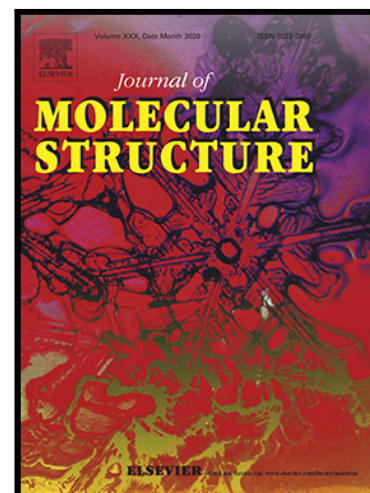


Journal Pre-proof

Silver nanoparticles supported on P, Se-codoped g-C₃N₄ nanosheet as a novel heterogeneous catalyst for reduction of nitroaromatics to their corresponding amines



Mohadese Piri , Majid M. Heravi , Ali Elhampour ,
Firouzeh Nemati

PII: S0022-2860(21)00779-1
DOI: <https://doi.org/10.1016/j.molstruc.2021.130646>
Reference: MOLSTR 130646

To appear in: *Journal of Molecular Structure*

Received date: 12 December 2020
Revised date: 4 May 2021
Accepted date: 5 May 2021

Please cite this article as: Mohadese Piri , Majid M. Heravi , Ali Elhampour , Firouzeh Nemati , Silver nanoparticles supported on P, Se-codoped g-C₃N₄ nanosheet as a novel heterogeneous catalyst for reduction of nitroaromatics to their corresponding amines, *Journal of Molecular Structure* (2021), doi: <https://doi.org/10.1016/j.molstruc.2021.130646>

This is a PDF file of an article that has undergone enhancements after acceptance, such as the addition of a cover page and metadata, and formatting for readability, but it is not yet the definitive version of record. This version will undergo additional copyediting, typesetting and review before it is published in its final form, but we are providing this version to give early visibility of the article. Please note that, during the production process, errors may be discovered which could affect the content, and all legal disclaimers that apply to the journal pertain.

© 2021 Elsevier B.V. All rights reserved.

Silver nanoparticles supported on P, Se-codoped g-C₃N₄ nanosheet as a novel heterogeneous catalyst for reduction of nitroaromatics to their corresponding amines

Mohadese Piri^a, Majid M. Heravi^{a,*}, m.heravi@alzahra.ac.ir, Ali Elhampour^{b,*},

Elhampour_ali@semnan.ac.ir, and Firouzeh Nemati^c

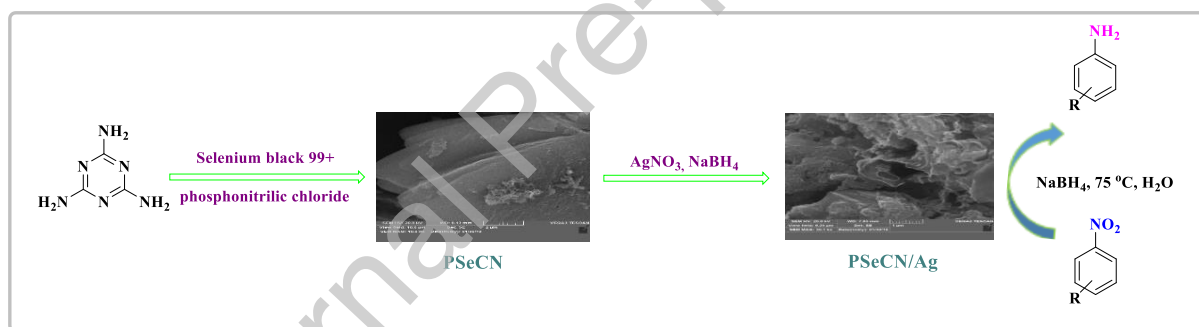
^aDepartment of Chemistry, School of Science, Alzahra University, Vanak, Tehran, Iran

^bLecturer, Semnan University, Semnan, Iran

^cDepartment of Chemistry, Semnan University, Semnan, Iran

*Corresponding authors

Graphical Abstract



Highlights

- Phosphorus and Selenium was doped into g-C₃N₄ by two-step calcination strategy.
- PSeCN/Ag was synthesized by the stabilization of Ag NPs on the surface of PSeCN.
- PSeCN/Ag exhibited excellent catalytic efficiency in the hydrogenation of nitroarenes.
- PSeCN/Ag can be recovered and reused six runs without appreciable loss in its activity.

Abstract

P, Se-codoped g-C₃N₄ (PSeCN) nanosheet was *in situ* prepared by facile thermal polymerization of melamine, phosphonitrilic chloride trimer, and selenium black powder as the precursors. It was found as a suitable support for the immobilization of silver nanoparticles (Ag NPs). The prepared nanocatalyst was fully characterized *via* standard analysis methods including EDX, ICP-OES, XRD, FT-IR, SEM, TEM, and BET. This PSeCN/Ag nanocatalyst with a higher specific surface area compared with CN, showed excellent catalytic activity towards the reduction of several nitroaromatic compounds using sodium borohydride (NaBH₄) in short reaction times with high efficiency and good selectivity in water as a green solvent. Significantly, the above-mentioned nanocomposite could be reused six times without appreciable loss of its catalytic activity.

Keywords

P, Se-codoped graphitic carbon nitride, heterogeneous nanocatalyst, Ag NPs, reduction, nitroarene

Introduction

In recent decades, due to industrial and economic growths, environmental pollution has always been strongly considered a serious concern, worldwide [1]. Organic pollutants have strong effects on the environment thus, should be intensively avoided [2-4]. Among the various pollutants, nitroaromatic compounds are the most common ones which are found in industrial and agricultural wastewaters [5].

The hydrogenation of toxic nitroarenes has been drawn much attention because the resultant aromatic amines are non-toxic and widely used as key intermediates and raw materials (major feedstocks) for the production of dyes, pigments, pharmaceuticals, herbicides, agrochemicals, and functional polymers [6-8].

There are several synthetic approaches reported in the chemical literature for the reduction of nitroarenes, such as electrolytic reduction [9], metal/acid reduction [10, 11], catalytic hydrogenation [12-15], etc.

The electrolytic processes are usually performed in alkaline or acidic media, requiring high energy consumption and the desired product yields are usually very low.

Metal/acid systems display poor selectivity and need strong acidic medium and stoichiometric amounts of reducing agents that eventually produce a large number of wastes, causing serious environmental problems (hence, are not economic and environmentally benign processes).

Among all known developed strategies, the catalytic hydrogenation of nitro compounds by noble metal nanoparticles (NMNPs) is a promising method as it can be carried out under mild reaction conditions, does not produce acid effluents, and demonstrates high selectivity and efficiency [16, 17].

Especially, the silver nanoparticles (Ag NPs), due to their biocompatibility, good conductivity, stability, high catalytic activity, anti-viral, antibacterial, and antifungal properties, and lower price as compared with other noble metals (Pt, Pd, Au) have attracted considerable attention in organic synthetic chemists community [18, 19]. However, free Ag NPs can easily agglomerate because of their high surface energy and small size, leading to poor durability and a remarkable decrease in catalytic efficiency. Immobilization of Ag NPs on the appropriate solid supports is an effective approach to circumvent these problems and thus enhance the catalytic activity and

stability. Toward this end, the design and synthesis of cost-effective and environmentally benign supports that can provide a good platform for stabilizing NMNPs are highly desirable.

In recent years, 2D materials have garnered significant attention [20], among them, 2D graphitic carbon nitride (g-C₃N₄), a metal-free polymeric semiconductor, with the layered structure and ultrahigh nitrogen content (theoretically up to 60 wt.%) has emerged as appealing catalyst support for the development of efficient and robust heterogeneous catalytic systems because of its dazzling advantages including unique optical, electronic and morphological peculiarities, high thermal and chemical stability, nontoxicity, abundant and cheap raw materials (ammonium thiocyanate, thiourea, urea, cyanamide, dicyandiamide, and melamine), and facile synthesis [21-24]. Unfortunately, despite these merits, applications of pure g-C₃N₄ in the catalysis are restricted by some disadvantages such as low specific surface area, low electrical conductivity, rapid carrier recombination rate, poor harvesting of the visible- light irradiation, weak π - π conjugated stacked structure, and lack of active sites [25-28].

Many innovative strategies have been developed to overcome these deficiencies such as protonating by strong acids [29], preparation of porous g-C₃N₄ [30], controlling morphology [31, 32], coupling with other semiconductors [33, 34], copolymerization [35, 36], and exfoliation to two-dimensional nanosheets [37]. The 2-D g-C₃N₄ nanosheets because of having a larger specific surface area than bulk g-C₃N₄ can improve catalytic activity. Also, heteroatom doping (e.g., B, F, S, P, and I) is an efficient and simple technique to tailor the electronic structures, chemical nature as well as texture properties, reduce the defect densities, improve catalytic performance and enhance active sites of g-C₃N₄ [38-40]. In particular, doping with two heteroatoms can significantly make more active sites to interact with immobilized nanoparticles than singularly doped ones [41].

Selenium is a metabolizable element in organisms and very eco-friendly and safe with exceptional and incomparable features within the periodic table [42]. Selenium possesses higher polarizability, facilitating charge localization, and larger atomic size than sulfur and lone pairs of selenium interact easily with the surrounding molecules. When Se is linked to metals, it indicates more metalline, resulting in excellent chemical stability [43, 44]. Therefore, it can be considered as an interesting candidate for doping into the framework of carbon nitrides. Also, P atom doping can increase the active sites of the carbon compounds [45]. Nonetheless, to the best of the authors' knowledge, there is no report in the literature about the co-doping of g-C₃N₄ with selenium and phosphorus heteroatoms.

In continuation of our studies on the design and synthesis of heterogeneous nanocatalysts [46-51] and armed with experience in the reduction of nitroaromatic compounds to their corresponding amines catalyzed by nanoparticles [52] in the present paper, we wish to report on our successful attempts of in situ preparation of P, Se-codoped g-C₃N₄ nanosheet (designated as PSeCN) by two-step calcination strategy using melamine, phosphonitrilic chloride trimer, and selenium black powder as the precursors and next used as the ideal support for the immobilization of Ag nanoparticles to obtain PSeCN/Ag. Taking into account all these considerations, the present study aimed to expand a highly efficient, robust, and easily separable nanocatalyst for the catalytic hydrogenation of nitroaromatic compounds in the aqueous media.

2. Experimental

2.1. Materials

Melamine, selenium black 99+, phosphonitrilic chloride trimer, silver nitrate, sodium borohydride, and various nitroarenes were purchased from Merck and used without any further purification.

2.2. Instrumentations

The formation of the nanocatalyst was confirmed by different identification techniques, such as Fourier transform infrared spectroscopy (FT-IR, Tensor IR 27 spectrometer) in the range of 4000-400 cm^{-1} , powder X-ray diffraction (XRD, Rigaku Ultima IV diffractometer under Cu-K α radiation at 2θ range of 10-90 $^\circ$), field-emission scanning electron microscopy (SEM, SIGMA VP), energy dispersive X-ray spectroscopy (EDX, Oxford instrument), transmission electron microscopy (TEM, CM30300Kv), and N $_2$ adsorption and desorption (BELSORP-mini II at the temperature of liquid nitrogen (77 K), and inductively coupled plasma optical emission spectroscopy (ICP-OES, DV 5300). Also, the promotion of the reaction was monitored by thin layer chromatography (TLC) on commercial aluminum-backed plates coated with layers of Merck silica gel 60 F254.

2.3. Preparation of nanocatalyst

2.3.1 Fabrication of P, Se-codoped g-C $_3$ N $_4$ (PSeCN) bulk

In a general synthesis route, melamine (2.8 g), phosphonitrilic chloride trimer (0.6 g), and selenium black powder (0.6 g) were thoroughly ground. The resulting mixture was placed in a ceramic crucible with a lid and pyrolyzed at 550 $^\circ\text{C}$ at a rate of 2 $^\circ\text{C min}^{-1}$ for 4 h. After cooling to ambient temperature, the synthesized product was repeatedly washed with deionized water and ethanol and put in an oven at 80 $^\circ\text{C}$ for 12 h to dry.

2.3.2 Fabrication of PSeCN nanosheets

The light yellow powder of the bulk P, Se-codoped g-C₃N₄ bulk was covered into P, Se-codoped g-C₃N₄ nanosheet through in situ thermal condensation at 600 °C at a rate of 5 °C min⁻¹ for 2 h. The prepared deep yellow powder was washed with deionized water and ethanol three times centrifuged repeatedly to eliminate impurities, then dried at 70 °C in the air for 12 h.

2.3.3 Fabrication of PSeCN/Ag nanocatalyst

To immobilize Ag NPs on PSeCN, PSeCN nanosheet (470 mg) was added to 100 mL of distilled water and sonicated. Then, aqueous AgNO₃ solution (4.72 mL, 10 mg.mL⁻¹) was added to the above suspension. After that, under ultrasonic, a solution of 210 mg NaBH₄ in H₂O (15 mL) was injected drop by drop and stirred continuously for 12 h in ambient temperature. Finally, the PSeCN/Ag was separated by centrifugation and dried in an oven for 24 h.

2.4. The catalytic activity of PSeCN/Ag in the reduction of nitroarenes

Typically, 4-nitroaniline (1 mmol), NaBH₄ as reducer (5 mmol), PSeCN/Ag nanocatalyst (20 mg) were added into a 10 mL vial containing 3 mL H₂O as the solvent. Then, the reaction mixture was stirred for a certain time at 75 °C. The reaction was checked by TLC. Upon the completion of the reaction, the PSeCN/Ag was isolated by centrifugation and washed with EtOH and H₂O to use for another consecutive run. Then, the product was extracted with ethyl acetate and purified by plate or column chromatography.

3. Results and discussion

3.1. Characterization

3.1.1. X-ray diffraction (XRD) studies

To study the crystallinity and phase structure of PSeCN and PSeCN/Ag, the XRD technique was conducted (Figure. 2). Both diffractograms reveal two prominent peaks at 2θ of 27.32° and

13.52° that are indexed as the (0 0 2) and (1 0 0) crystal planes of graphitic materials, corresponding to the interlayer structural packing and in-plane repeated tri-s-triazine units, respectively [53]. These results show that the original structure of g-C₃N₄ was preserved after P and Se co-doping. Also, the absence of peaks related to Se and P indicates that these elements have entered into the g-C₃N₄ network. After loading Ag, other obvious diffraction peaks appear in the XRD pattern of PSeCN/Ag, at 2θ = 38.6°, 44.32°, 64.34°, and 77° corresponding to (1 1 1), (2 0 0), (2 2 0), (3 1 1) diffractions of the face-centered-cubic structure of Ag nanoparticles [54]. As a result, Ag nanoparticles have been successfully assembled on the surface of the PSeCN.

<Figure 1>

3.1.2. Fourier transform spectroscopy (FT-IR) studies

To obtain information about the chemical structure of the synthesized specimens, FT-IR analysis was performed. The FT-IR spectra of g-C₃N₄, PSeCN (nano), PSeCN/Ag present similar absorption bands which confirm the formation of the graphitic structure of carbon nitride in all samples, as shown in Figure 1. For all samples, the absorption bands at 807 and 885 cm⁻¹ belong to the out-of-plane bending modes of heptazine units and the cross-linked deformation mode of N-H bonds, respectively [55]. The peaks at 1238 and 1319 cm⁻¹ correspond to the stretching vibration of connected units of C-N(-C)-C or C-NH-C [56]. The observed absorption peaks in 1407, 1560, and 1640 cm⁻¹ are assigned to the stretching vibrations of C-N and C=N in heterocycles (in tri-s-triazine rings) [57]. The broad band located at 3000-3500 cm⁻¹ is attributed to the O-H and N-H stretching vibration modes possibly due to absorbed water molecules and

uncondensed amino groups [58]. No characteristic peaks related to covalent bonding of P and Se with other elements were detected in the spectrum of PSeCN, possibly owing to overlap with the vibration mode of C-N and low doping levels of P and Se. Also, the FT-IR spectrum of PSeCN/Ag is similar to PSeCN, suggesting that the structure of the prepared nanocatalyst remains unchanged after the deposition of Ag nanoparticles.

<Figure 2>

3.1.3. Scanning electron microscopy (SEM) studies

SEM images of the PSeCN and PSeCN/Ag elucidated their surface morphology and nanostructure (Figure. 3). The SEM images of PSeCN exhibit plate-like structures with smoothed surfaces (Figure. 3a and b). After the deposition of Ag NPs, the morphology did not affect but a rough surface was observed (Figure. 3c and d) [59, 60].

<Figure 3>

3.1.4. Energy dispersive X-ray spectroscopy (EDX) studies

EDX analysis was applied to determine the chemical composition of PSeCN/Ag nanocatalyst (Figure. 4). The presence of various elements such as C, N, P, Se, and Ag in the EDX spectrum of PSeCN/Ag confirm the successful doping of P and Se in PSeCN as well as the deposition of Ag NPs on the surface of the PSeCN/Ag.

<Figure 4>

3.1.5 Elemental mapping analysis

To further investigate the elemental composition and distribution in PSeCN/Ag, the EDX-mapping analysis was carried out (Figure. 5). The map images also affirm the presence of C, N, P, Se, and Ag elements, which are homogeneously distributed in the structure PSeCN/Ag.

<Figure 5>

3.1.6 Transmission electron microscopy (TEM) studies

The surface structures and morphology of the PSeCN/Ag nanocatalyst were further examined using TEM. As shown in Figure 6, the lighter parts can be assigned to the sheet-like morphology of PSeCN with lower density and the darker spots correspond to Ag NPs with higher density. The Ag NPs have a spherical morphology and are uniformly dispersed over the PSeCN sheets without aggregation.

<Figure 6>

3.1.7 Inductively coupled plasma-optical emission spectrometer (ICP- OES) analysis

In the following, ICP-OES analysis was exploited to determine the exact content of Ag in the nanocatalyst. The loading amount of Ag in the PSeCN/Ag is reported to be 2.69% that is in good agreement with the EDX analysis result.

3.1.8. Nitrogen adsorption-desorption analysis

To evaluate the textural and structural features in the as-fabricated samples, nitrogen sorption analysis was performed. The N₂ adsorption and desorption diagrams of PSeCN bulk, PSeCN nano, and PSeCN/Ag are presented in Figure.7. Also, the specific surface area, pore size, and pore volume are listed in Table 1. N₂ adsorption-desorption diagram of all samples displays a type IV curve based on the IUPAC standard which confirms the mesoporous structure. As

expected, the specific surface area of PSeCN bulk ($9.64 \text{ m}^2 \text{ g}^{-1}$) is nearly 4 times larger than that of PSeCN nano ($33.61 \text{ m}^2 \text{ g}^{-1}$). The higher specific surface area can provide more active sites and increase catalytic performance. Besides, the PSeCN/Ag exhibits a lower specific surface area compared to PSeCN. Decreasing the surface area of PSeCN/Ag indicates that the Ag NPs were successfully anchored on the surface of PSeCN and filled the most often pores.

<Figure 7>

Table 1. Summary of BET measurements

Sample	Pore volume ($\text{cm}^3 \cdot \text{g}^{-1}$)	Specific surface area ($\text{m}^2 \cdot \text{g}^{-1}$)	Pore size (nm)
PSeCN(bulk)	0.074	9.64	16.64
PSeCN(nano)	0.174	33.61	14.56
PSeCN/Ag	0.118	20.39	16.49

3.2 Evaluation of the catalytic activity of PSeCN/Ag

To extend the utilization of PSeCN/Ag nanocatalyst in different aromatic nitro compounds catalytic reduction, its catalytic potential was examined in the reduction reaction of 4-nitroaniline using NaBH_4 as the reductant. For the optimization of the reaction conditions, the influence of different parameters (dosage of the catalyst and reductant, solvent, and temperature) was surveyed in detail. Firstly, various quantities of the catalyst were tested (Table 2, entries 1-4). Entry 1 displays that in the absence of a catalyst, the reduction reaction cannot occur. Thus, PSeCN/Ag is an essential factor for this reaction. As can be seen, 20 mg of catalyst is the most

appropriate amount (Table 2, entry 3). When the optimal amount of catalyst was obtained, the NaBH_4 loading was examined. With the decrease of the NaBH_4 amount from 5 to 4 mmol, a decrease in the product yield was observed (Table 2, entry 5). Next, temperature screening was undertaken and $75\text{ }^\circ\text{C}$ proved to be the optimum reaction temperature. When the reaction temperature was reduced to $55\text{ }^\circ\text{C}$ the product yield decreased to 60% and increase the reaction temperature to $95\text{ }^\circ\text{C}$ did not have a positive effect (appreciable influence) on the product conversion percentage and rate of reaction (Table 2, entries 6 and 7). Finally, to assess the solvent effect, the test reaction was performed in various solvents (Table 2, entries 8 and 9). Among them, water, as a sustainable, cheap, and green solvent, exhibited the best performance with 98% yield.

Therefore, the optimal reaction conditions were determined to be PSeCN/Ag nanocatalyst (20 mg) and NaBH_4 (5 mmol) at $75\text{ }^\circ\text{C}$ in H_2O as solvent (Table 2, entry 3).

Table 2. Optimization of reaction conditions^a.

Entry	Catalyst (mg)	NaBH_4 (mmol)	Solvent	Temp.($^\circ\text{C}$)	Time(min)	Yield(%) ^b
1	-	5	H_2O	75	25	-
2	10	5	H_2O	75	25	75
3	20	5	H_2O	75	25	99
4	30	5	H_2O	75	25	98
5	20	4	H_2O	75	25	99
6	20	5	H_2O	55	25	60
7	20	5	EtOH	95	25	98

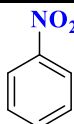
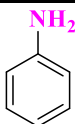
8	20	5	EtOH: H ₂ O (1:1)	75	25	83
9	20	5	EtOH	75	25	90

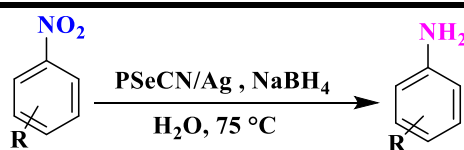
^aReaction condition: 4-nitro aniline (1.0 mmol), NaBH₄, solvent (3 mL).

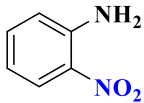
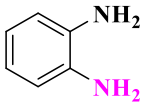
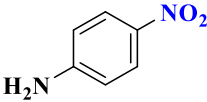
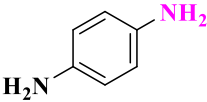
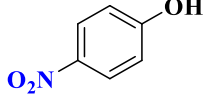
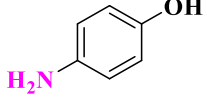
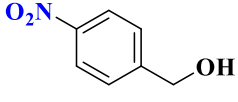
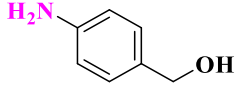
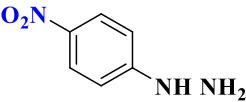
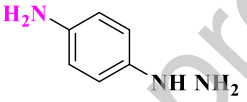
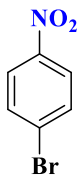
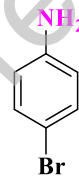
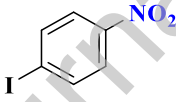
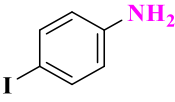
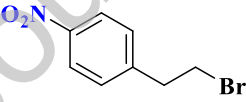
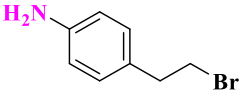
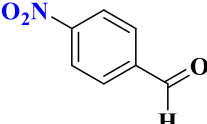
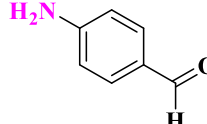
^bIsolated yield.

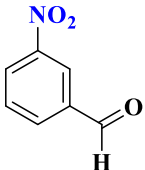
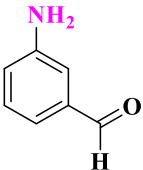
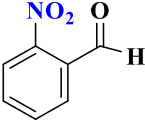
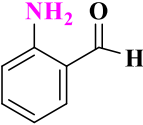
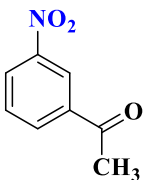
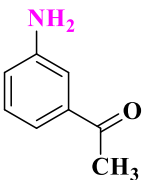
To confirm the general applicability of PSeCN/Ag, the reduction of a variety of nitroarenes was investigated under the optimum conditions, and outcomes are summarized in Table 3. Starting materials having electron-rich groups such as NH₂, OH, CH₂OH, and NHNH₂, and electron-poor groups like I, Br, Cl, and CF₃ were transformed into the relevant amines products with good to excellent yields and selectively and no dehalogenated product was seen in halogenated nitroarenes. More importantly, the aromatic nitro compounds bearing the challenging reducible functional groups, including ketone and aldehyde were effectively converted into their corresponding aniline derivatives with high selectivity and carbonyl groups remained unchanged during the reduction process.

Table 3. Reduction of nitroarenes using PSeCN/Ag nanocatalyst^a

Entry	Substrate	Product	Time (min)	Yield (%)
1			25	99



2			50	99
3			20	99
4			25	98
5			120	95
6			110	98
7			120	92
8			100	90
9			110	76
10			120	85

11			180	83
12			110	84
13			165	74

Reaction conditions: 4-nitroaniline (1 mmol), catalyst (20 mg), NaBH₄ (5 mmol), solvent (3 mL), temperature (75°C).

3.3 Reusability of the catalyst

Finally, a reusability test was accomplished to explore the industrial applicability and sustainability of the fabricated nanocatalyst. For this purpose, the catalyst was isolated at the end of the reaction by centrifugation and reused in the next runs under identical conditions after washing frequently with warm methanol and drying in an oven. The yield of the product slightly reduced from 99 to 91% after six runs (Figure. 8). This result demonstrates that there is no significant degradation in the catalytic activity of PSeCN/Ag. However, in run 7, the conversion percentage of the product decreased to 85%.

<Figure 8>

4. Conclusion

In conclusion, the present study focused on the g-C₃N₄ modification using three efficient techniques such as phosphorus and selenium co-doping, creating mesoporous construction (sheet-like structure), and immobilization of Ag NPs on its surface. In situ phosphorus and selenium co-doped graphitic carbon nitride nanosheet (PSeCN) was successfully prepared for the first time by applying melamine, phosphonitrilic chloride trimer, and selenium black powder as precursors through facile thermal polymerization strategy (method) and used as an excellent platform for stabilization of Ag NPs. Then, synthesized PSeCN/Ag was exploited as a heterogeneous nanocatalyst for promoting the reduction of aromatic nitro compounds in aqueous media and indicated remarkable catalytic efficacy and selectivity. The outstanding performance of PSeCN/Ag could be ascribed to two factors. First, attendance of support with nanometer size. Secondly, 2-D confinement offers more active sites. Additionally, nanocatalyst could be easily recovered and reused for five runs with negligible loss in its activity because of the strong interaction of PSeCN with Ag NPs. Hopefully, this study would provide enormous opportunities for the design and synthesis of other metal-based heteroatom-doped g-C₃N₄ materials for the advanced hydrogenation process with challenging compounds.

Credit Author Statement

Mohadese Piri (Investigation, Data Curation, Visualization)

Majid M. Heravi (Conceptualization; Validation, Resources, Writing - Review & Editing, Supervision, Project administration, Funding acquisition)

Ali Elhampour (Conceptualization, Methodology, Data Curation, Writing - Original Draft)

Firouzeh Nemati (Conceptualization, Supervision)

Declaration of interests

There are no conflicts to declare.

Acknowledgments

The authors are thankful from Alzahra University Research Council for financial support. MMH also appreciates the granted individual research chair given by Iran National Scientific Foundation (INSF).

References

- [1] Y.-C. Chang, D.-H. Chen, Catalytic reduction of 4-nitrophenol by magnetically recoverable Au nanocatalyst, *J. Hazard. Mater.*, 165 (2009) 664-669.
- [2] C. Yu, Z. Wu, R. Liu, D.D. Dionysiou, K. Yang, C. Wang, H. Liu, Novel fluorinated Bi₂MoO₆ nanocrystals for efficient photocatalytic removal of water organic pollutants under different light source illumination, *Appl. Catal. B., Environ.*, 209 (2017) 1-11.
- [3] Y. Choi, M.S. Koo, A.D. Bokare, D.-h. Kim, D.W. Bahnemann, W. Choi, Sequential process combination of photocatalytic oxidation and dark reduction for the removal of organic pollutants and Cr (VI) using Ag/TiO₂, *Environ. Sci. Technol.*, 51 (2017) 3973-3981.
- [4] O.M. Wani, M. Safdar, N. Kinnunen, J. Jänis, Dual effect of manganese oxide micromotors: catalytic degradation and adsorptive bubble separation of organic pollutants, *Chem. Eur. J.*, 22 (2016) 1244-1247.
- [5] H. Guo, X. Yan, Y. Zhi, Z. Li, C. Wu, C. Zhao, J. Wang, Z. Yu, Y. Ding, W. He, Nanostructuring gold wires as highly durable nanocatalysts for selective reduction of nitro compounds and azides with organosilanes, *Nano Res.*, 8 (2015) 1365-1372.

- [6] H. Huang, X. Liang, X. Wang, Y. Sheng, C. Chen, X. Zou, X. Lu, N-doped graphitic carbon-improved Co-MoO₃ catalysts on ordered mesoporous SBA-15 for chemoselective reduction of nitroarenes, *Appl. Catal. A*, 559 (2018) 127-137.
- [7] X. Cui, K. Liang, M. Tian, Y. Zhu, J. Ma, Z. Dong, Cobalt nanoparticles supported on N-doped mesoporous carbon as a highly efficient catalyst for the synthesis of aromatic amines, *J. Colloid Interface Sci*, 501 (2017) 231-240.
- [8] M. Gholinejad, F. Zareh, C. Nájera, Nitro group reduction and Suzuki reaction catalysed by palladium supported on magnetic nanoparticles modified with carbon quantum dots generated from glycerol and urea, *Appl. Organomet. Chem*, 32 (2018) e3984.
- [9] C. Lagrost, L. Preda, E. Volanschi, P. Hapiot, Heterogeneous electron-transfer kinetics of nitro compounds in room-temperature ionic liquids, *J. Electroanal. Chem*, 585 (2005) 1-7.
- [10] F.A. Khan, J. Dash, C. Sudheer, R.K. Gupta, Chemoselective reduction of aromatic nitro and azo compounds in ionic liquids using zinc and ammonium salts, *Tetrahedron Lett*, 44 (2003) 7783-7787.
- [11] G. Rai, J.M. Jeong, Y.-S. Lee, H.W. Kim, D.S. Lee, J.-K. Chung, M.C. Lee, Ionic liquid mediated efficient reduction of nitroarenes using stannous chloride under sonication, *Tetrahedron Lett*, 46 (2005) 3987-3990.
- [12] F. Figueras, B. Coq, Hydrogenation and hydrogenolysis of nitro-, nitroso-, azo-, azoxy- and other nitrogen-containing compounds on palladium, *J. Mol. Catal., A. Chem*, 173 (2001) 223-230.
- [13] S.M. Sajadi, M. Nasrollahzadeh, M. Maham, Aqueous extract from seeds of *Silybum marianum* L. as a green material for preparation of the Cu/Fe₃O₄ nanoparticles: a magnetically recoverable and reusable catalyst for the reduction of nitroarenes, *J. Colloid Interface Sci*, 469 (2016) 93-98.
- [14] X. Tan, Z. Zhang, Z. Xiao, Q. Xu, C. Liang, X. Wang, Organic-inorganic hybrid SiO₂ supported gold nanoparticles: facile preparation and catalytic hydrogenation of aromatic nitro compounds, *Catalysis Lett*, 142 (2012) 788-793.
- [15] Y. Zheng, K. Ma, H. Wang, X. Sun, J. Jiang, C. Wang, R. Li, J. Ma, A green reduction of aromatic nitro compounds to aromatic amines over a novel Ni/SiO₂ catalyst passivated with a gas mixture, *Catalysis Lett*, 124 (2008) 268-276.
- [16] X. Qiu, Q. Liu, M. Song, C. Huang, Hydrogenation of nitroarenes into aromatic amines over Ag@BCN colloidal catalysts, *J. Colloid Interface Sci*, 477 (2016) 131-137.
- [17] S.M. Alshehri, T. Almuqati, N. Almuqati, E. Al-Farraj, N. Alhokbany, T. Ahamad, Chitosan based polymer matrix with silver nanoparticles decorated multiwalled carbon nanotubes for catalytic reduction of 4-nitrophenol, *Carbohydr. polym*, 151 (2016) 135-143.

- [18] X. Cui, H. Li, M. Yuan, J. Yang, D. Xu, Z. Li, G. Yu, Y. Hou, Z. Dong, Facile preparation of fluffy N-doped carbon modified with Ag nanoparticles as a highly active and reusable catalyst for catalytic reduction of nitroarenes, *J. Colloid Interface Sci*, 506 (2017) 524-531.
- [19] A. Rostami-Vartooni, M. Nasrollahzadeh, M. Alizadeh, Green synthesis of seashell supported silver nanoparticles using *Bunium persicum* seeds extract: application of the particles for catalytic reduction of organic dyes, *J. Colloid Interface Sci*, 470 (2016) 268-275.
- [20] A. U. Ammar, I. D. Yildirim, F. Bakan, E. Erdem, ZnO and MXenes as electrode materials for supercapacitor devices, *Beilstein J. Nanotechnol*, 12 (2021) 49-57.
- [21] J. Sun, Y. Fu, G. He, X. Sun, X. Wang, Green Suzuki-Miyaura coupling reaction catalyzed by palladium nanoparticles supported on graphitic carbon nitride, *Appl. Catal. B., Environ*, 165 (2015) 661-667.
- [22] N. Azizi, E. Farhadi, Magnetically separable g-C₃N₄ hybrid nanocomposite: Highly efficient and eco-friendly recyclable catalyst for one-pot synthesis of α -aminonitriles, *Appl. Organomet. Chem*, 32 (2018) e4188.
- [23] Q. Liang, M. Zhang, C. Liu, S. Xu, Z. Li, Sulfur-doped graphitic carbon nitride decorated with zinc phthalocyanines towards highly stable and efficient photocatalysis, *Appl. Catal. A*, 519 (2016) 107-115.
- [24] Y. Rangraz, F. Nemati, A. Elhampour, Selenium-doped graphitic carbon nitride decorated with Ag NPs as a practical and recyclable nanocatalyst for the hydrogenation of nitro compounds in aqueous media, *Appl. Surf. Sci*, 507 (2020) 145164.
- [25] A. Mohammad, M.E. Khan, M.H. Cho, Sulfur-doped-graphitic-carbon nitride (Sg-C₃N₄) for low cost electrochemical sensing of hydrazine, *J. Alloys. Compd*, 816 (2020) 152522.
- [26] A. Mohammad, M.E. Khan, M.R. Karim, M.H. Cho, Synergistically effective and highly visible light responsive SnO₂-g-C₃N₄ nanostructures for improved photocatalytic and photoelectrochemical performance, *Appl. Surf. Sci*, 495 (2019) 143432.
- [27] S. Sadjadi, M. Malmir, M.M. Heravi, Preparation of Ag-doped g-C₃N₄ Nano Sheet Decorated Magnetic γ -Fe₂O₃@SiO₂ Core-Shell Hollow Spheres through a Novel Hydrothermal Procedure: Investigation of the Catalytic activity for A³, KA² Coupling Reactions and [3+ 2] Cycloaddition, *Appl. Organomet. Chem*, 32 (2018) e4413.
- [28] S. Sadjadi, M. Malmir, M.M. Heravi, F.G. Kahangi, Magnetic covalent hybrid of graphitic carbon nitride and graphene oxide as an efficient catalyst support for immobilization of Pd nanoparticles, *Inorganica Chim. Acta*, 488 (2019) 62-70.
- [29] Y. Zhang, A. Thomas, M. Antonietti, X. Wang, Activation of carbon nitride solids by protonation: morphology changes, enhanced ionic conductivity, and photoconduction experiments, *J. Am. Chem. Soc*, 131 (2009) 50-51.

- [30] F. Goettmann, A. Fischer, M. Antonietti, A. Thomas, Chemical synthesis of mesoporous carbon nitrides using hard templates and their use as a metal-free catalyst for Friedel–Crafts reaction of benzene, *Angew. Chem*, 45 (2006) 4467-4471.
- [31] Y. Zheng, L. Lin, X. Ye, F. Guo, X. Wang, Helical graphitic carbon nitrides with photocatalytic and optical activities, *Angew. Chem*, 53 (2014) 11926-11930.
- [32] Y. Cui, G. Zhang, Z. Lin, X. Wang, Condensed and low-defected graphitic carbon nitride with enhanced photocatalytic hydrogen evolution under visible light irradiation, *Appl. Catal. B. Environ*, 181 (2016) 413-419.
- [33] P. Xia, B. Zhu, B. Cheng, J. Yu, J. Xu, 2D/2D g-C₃N₄/MnO₂ nanocomposite as a direct Z-scheme photocatalyst for enhanced photocatalytic activity, *ACS Sustain. Chem. Engin*, 6 (2018) 965-973.
- [34] S. Obregón, G. Colón, Improved H₂ production of Pt-TiO₂/g-C₃N₄-MnO_x composites by an efficient handling of photogenerated charge pairs, *Appl. Catal. B. Environm*, 144 (2014) 775-782.
- [35] W. Ho, Z. Zhang, W. Lin, S. Huang, X. Zhang, X. Wang, Y. Huang, Copolymerization with 2, 4, 6-triaminopyrimidine for the rolling-up the layer structure, tunable electronic properties, and photocatalysis of g-C₃N₄, *ACS appl. Mater. Interfaces*, 7 (2015) 5497-5505.
- [36] Y. Ishida, L. Chabanne, M. Antonietti, M. Shalom, Morphology control and photocatalysis enhancement by the one-pot synthesis of carbon nitride from preorganized hydrogen-bonded supramolecular precursors, *Langmuir*, 30 (2014) 447-451.
- [37] L. Chen, J.-T. Ren, Z.-Y. Yuan, Atomic heterojunction-induced electron interaction in P-doped g-C₃N₄ nanosheets supported V-based nanocomposites for enhanced oxidative desulfurization, *Chem. Eng. J*, 387 (2020) 124164.
- [38] L. Jiang, X. Yuan, Y. Pan, J. Liang, G. Zeng, Z. Wu, H. Wang, Doping of graphitic carbon nitride for photocatalysis: a review, *Appl. Catal. B. Environ*, 217 (2017) 388-406.
- [39] W.-J. Ong, L.-L. Tan, Y.H. Ng, S.-T. Yong, S.-P. Chai, Graphitic carbon nitride (g-C₃N₄)-based photocatalysts for artificial photosynthesis and environmental remediation: are we a step closer to achieving sustainability, *Chem. Rev*, 116 (2016) 7159-7329.
- [40] C. Hu, W.-Z. Hung, M.-S. Wang, P.-J. Lu, Phosphorus and sulfur codoped g-C₃N₄ as an efficient metal-free photocatalyst, *Carbon*, 127 (2018) 374-383.
- [41] Q. Liu, J. Fan, Y. Min, T. Wu, Y. Lin, Q. Xu, B. N-codoped graphene nanoribbons supported Pd nanoparticles for ethanol electrooxidation enhancement, *J. Mater. Chem. A*, 4 (2016) 4929-4933.
- [42] F. Qiao, J. Wang, S. Ai, L. Li, As a new peroxidase mimetics: The synthesis of selenium doped graphitic carbon nitride nanosheets and applications on colorimetric detection of H₂O₂ and xanthine, *Sens. Actuator. B-Chem*, 216 (2015) 418-427.

- [43] W. Wang, Y. Dong, L. Xu, W. Dong, X. Niu, Z. Lei, Combining Bimetallic-Alloy with Selenium Functionalized Carbon to Enhance Electrocatalytic Activity towards Glucose Oxidation, *Electrochim. Acta*, 244 (2017) 16-25.
- [44] B. Fahimirad, Y. Rangraz, A. Elhampour, F. Nemati, Diphenyl diselenide grafted onto a Fe_3O_4 -chitosan composite as a new nanosorbent for separation of metal ions by effervescent salt-assisted dispersive magnetic micro solid-phase extraction, *Microchim. Acta*, 185 (2018) 560.
- [45] K. Yu, Y. Lin, J. Fan, Q. Li, P. Shi, Q. Xu, Y. Min, Ternary N, S, and P-Doped Hollow Carbon Spheres Derived from Polyphosphazene as Pd Supports for Ethanol Oxidation Reaction, *Catalysts*, 9 (2019) 114.
- [46] T. Tamoradi, M. Daraie, M.M. Heravi, Synthesis of palladated magnetic nanoparticle ($\text{Pd}@\text{Fe}_3\text{O}_4/\text{AMOCOA}$) as an efficient and heterogeneous catalyst for promoting Suzuki and Sonogashira cross-coupling reactions, *Appl. Organomet. Chem*, n/a e5538.
- [47] L. Mohammadi, M.M. Heravi, S. Sadjadi, M. Malmir, Hybrid of Graphitic Carbon Nitride and Palladated Magnetic Carbon Dot: An Efficient Catalyst for Coupling Reaction, *ChemistrySelect*, 4 (2019) 13404-13411.
- [48] S. Sadjadi, F. Ghoreyshi Kahangi, M.M. Heravi, Pd stabilized on nanocomposite of halloysite and β -cyclodextrin derived carbon: An efficient catalyst for hydrogenation of nitroarene, *Polyhedron*, 175 (2020) 114210.
- [49] S. Sadjadi, G. Lazzara, M.M. Heravi, G. Cavallaro, Pd supported on magnetic carbon coated halloysite as hydrogenation catalyst: Study of the contribution of carbon layer and magnetization to the catalytic activity, *Appl. Clay. Sci*, 182 (2019) 105299.
- [50] S. Sadjadi, M.M. Heravi, Pd@tetrahedral hollow magnetic nanoparticles coated with N-doped porous carbon as an efficient catalyst for hydrogenation of nitroarenes, *Appl. Organomet. Chem*, 33 (2019) e5229.
- [51] M. Daraie, M.M. Heravi, SMA/Py/ZnO as a new biocompatible polymer supported nanocatalyst for the synthesis of chromeno[2,3-d] pyrimidine-diones through a novel and efficient pathway, *Can. J. Chem*, 97 (2019) 772-779.
- [52] R. Sedghi, M. M Heravi, S. Asadi, N. Nazari, M. R Nabid, Recently used nanocatalysts in reduction of nitroarenes, *Curr. Org. Chem*, 20 (2016) 696-734.
- [53] S. Panneri, M. Thomas, P. Ganguly, B.N. Nair, A.P. Mohamed, K.G.K. Warriar, U.S. Hareesh, C_3N_4 anchored ZIF 8 composites: photo-regenerable, high capacity sorbents as adsorptive photocatalysts for the effective removal of tetracycline from water, *Catal. Sci. Technol*, 7 (2017) 2118-2128.
- [54] A. Elhampour, F. Nemati, M.M. Heravi, Nano Ag-doped magnetic- Fe_3O_4 @mesoporous TiO_2 core-shell hollow spheres: synthesis and enhanced catalytic activity in A^3 and KA^2 coupling reactions, *Monatsh. Chemie*, 148 (2017) 1793-1805.

[55] V. Balakumar, H. Kim, J.W. Ryu, R. Manivannan, Y.-A. Son, Uniform assembly of gold nanoparticles on S-doped g-C₃N₄ nanocomposite for effective conversion of 4-nitrophenol by catalytic reduction, *J. Mater. Sci. Technol*, 40 (2020) 176-184.

[56] H. Wang, Y. Wang, Y. Guo, X.-K. Ren, L. Wu, L. Liu, Z. Shi, Y. Wang, Pd nanoparticles confined within triazine-based carbon nitride NTs: An efficient catalyst for Knoevenagel condensation-reduction cascade reactions, *Catal. Today*, 330 (2019) 124-134.

[57] J. Liu, T. Zhang, Z. Wang, G. Dawson, W. Chen, Simple pyrolysis of urea into graphitic carbon nitride with recyclable adsorption and photocatalytic activity, *J. Mater. Chem*, 21 (2011) 14398-14401.

[58] Y. Wang, J. Zhang, X. Wang, M. Antonietti, H. Li, Boron- and Fluorine-Containing Mesoporous Carbon Nitride Polymers: Metal-Free Catalysts for Cyclohexane Oxidation, *Angew. Chem., Int. Ed.*, 49 (2010) 3356.

[59] S. B. Patel, D. V. Vasava, Synthesis and Characterization of Ag@g-C₃N₄ and Its Photocatalytic Evolution in Visible Light Driven Synthesis Of Ynone. *ChemCatChem*, 2 (2020) 631.

[60] S. B. Patel, D. V. Vasava. Carbon Nitride-Supported Silver Nanoparticles: Microwave-Assisted Synthesis of Propargylamine and Oxidative C-C Coupling Reaction. *ChemistrySelect*. 2 (2018) 471.

Figure 1. XRD patterns of (a) PSeCN and (b) PSeCN/Ag

Figure 2. FT-IR spectra of (a) g-C₃N₄, (b) PSeCN (nano), and (c) PSeCN/Ag

Figure 3. SEM images of (a, b) PSeCN (nano), and (c, d) PSeCN/Ag

Figure 4. EDX spectrum of PSeCN/Ag

Figure 5. Elemental mapping data of PSeCN/Ag

Figure 6. TEM images of PSeCN/Ag

Figure 7. N₂ adsorption and desorption diagrams of (a) PSeCN bulk, (b) PSeCN nano, (c) PSeCN/Ag

Figure 8. Catalyst recycling diagram

Journal Pre-proof